

Green Open Access:

Authors' Self-archive manuscript

(enabled to public access on **04.11.2018**, after 24 month embargo period)

This manuscript was published as formal in:

Tetrahedron 72 (2016) 8215e8222

<http://dx.doi.org/10.1016/j.tet.2016.10.052>

<https://www.sciencedirect.com/science/article/pii/S0040402016311115>



Pyridyl-indolizine derivatives as DNA binders and pH-sensible fluorescent dyes

Narcisa-Laura Marangoci^a, Lacramioara Popovici^b, Elena-Laura Ursu^a, Ramona Danac^b, Lilia Clima^a,
Corneliu Cojocaruc^c, Adina Coroaba^a, Andrei Neamtu^d, Ionel Mangalagiu^b, Mariana Pinteala^a and
Alexandru Rotaru^{a,*}

^a“Petru Poni” Institute of Macromolecular Chemistry, Romanian Academy, Centre of Advanced Research in
Bionanoconjugates and Biopolymers, Aleea Grigore Ghica Voda 41 A, 700487 Iasi, Romania.

^bAlexandru Ioan Cuza University of Iasi, Chemistry Department, 14 Carol I, Iasi 700506, Romania.

^c“Petru Poni” Institute of Macromolecular Chemistry, Romanian Academy, Department of Inorganic
Polymers, Aleea Grigore Ghica Voda 41 A, 700487 Iasi, Romania.

^d“Gr.T. Popa” University of Medicine and Pharmacy of Iasi, 16, University Street, 700115 Iasi, Romania.

1. Introduction

The development of small organic molecules capable of binding to specific biomolecules or used in biomedical optical imaging has recently received enormous attention.¹ When it comes to nucleic acid binders, the most attractive reason of the research seems to be the well-established fact that many therapeutic agents, particularly anticancer drugs, interact with nucleic acids via noncovalent binding motifs, such as intercalations between base pairs, minor/major groove binding and outside binding with self-stacking along the DNA skeleton.² The search for properly designed organic molecules able to interact efficiently with nucleic acids is therefore, still of crucial importance. On the other hand, small organic molecules with peculiar emission properties can not only be used to bind biomolecules but, depending on the molecular structure, can also act as an indicator to determine intrinsically nonfluorescent parameters such as, for example, pH value. In this case, their fluorescence properties could respond to the temporal chemical composition of the biological environment. Even though organic dyes such as BODIPY, rhodamine, fluorescein, coumarin and cyanine derivatives have been widely used in bioimaging, biosensing, medical diagnosis, and environmental detection³, an important feature that constrains many interesting fluorophores for their full potential applications is their undesirable photophysical properties. For instance, many bright organic dyes usually have the serious disadvantage of very small *Stokes* shifts (typically less than 25-30 nm), which can lead to serious self-quenching and fluorescence detection errors because of excitation backscattering effects. Earlier, we have reported the first three-component one-pot synthesis of highly fluorescent 7-(pyridin-4-yl)-substituted indolizines with a considerable large *Stokes* shift and their preliminary pH-dependent emission properties in organic solvents.⁴ Recent reports have also shown the successful synthesis and structure-emissions properties studies of the indolizine-based fluorescent platforms named Seoul-Fluor⁵ showing the strong potential of indolizine derivatives for the applications in bioimaging and biosensing. On the basis of our previous studies and recent advances in the applications of indolizine-based derivatives, we envisioned that the unique features of pyridine-indolizines and their planar structure could lead to new applications as nucleic acid binders or pH-sensible dye. Toward this goal, we have started to investigate the DNA binding properties of our molecules by variation of the specific substituents in the indolizinic ring. In particular, we have designed a synthetic route to introduce anthracene moiety to indolizinic skeleton to enhance the binding affinity to nucleic acids due to the anthracene well-known electro-optical properties and rigid aromatic panels capable of fostering various aromatic interactions providing ideal structural interactions within the helical framework of DNA.⁶ Additionally, we have investigated the differences in nucleic acid binding properties of both final anthracene containing 7-(pyridin-4-yl)-substituted indolizine and its precursor containing only pyridyl-indolizine moiety to better understand the influence of anthracene substituent in nucleic acid binding mechanism.

In this work we report on the synthesis, particular fluorescence properties in aqueous buffer solutions at different pH values, as well as preliminary evaluation of pyridyl-indolizine containing anthracene moiety as potential DNA binding agent (Fig. 1). We have also correlated the obtained experimental data on the affinity of the anthracene-based indolizinic compound and its non-anthracene precursor toward nucleic acids with the theoretical docking simulations.

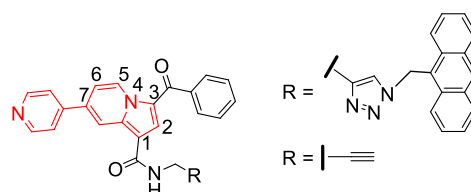


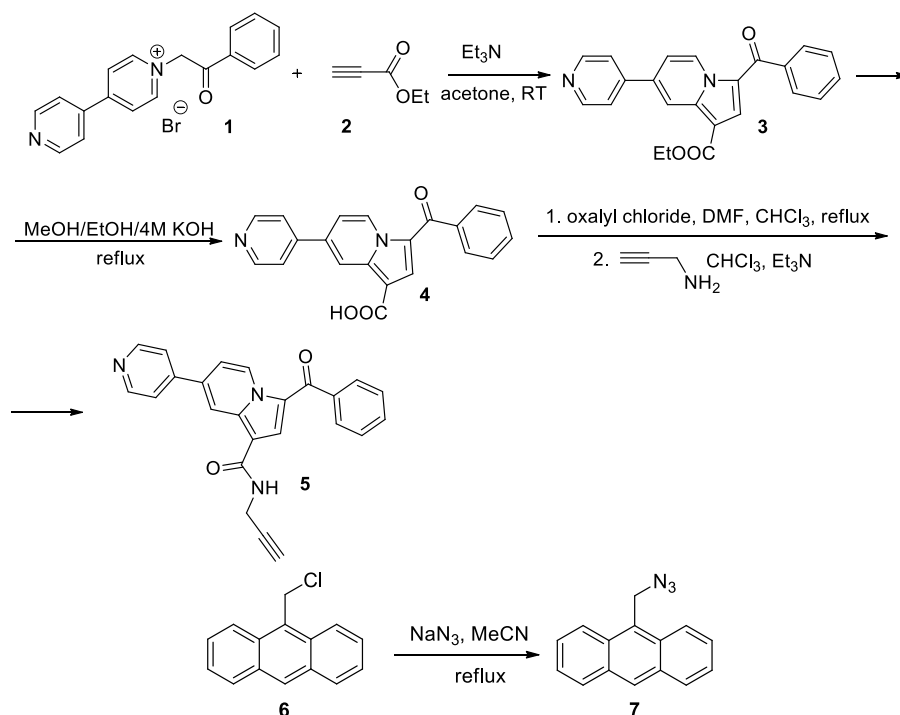
Fig.1. Structure of the studied pyridyl-indolizines containing an anthracene moiety and its precursor.

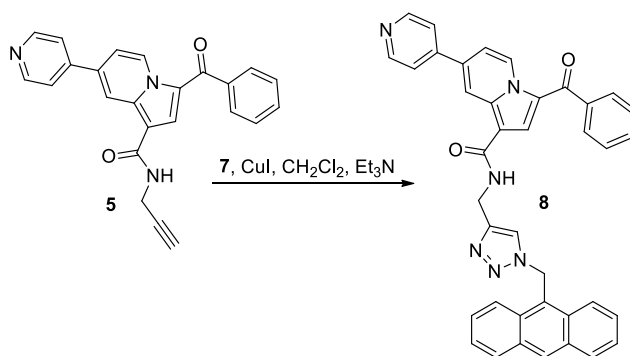
The appendix of anthracenyl group was achieved by exploiting the position 1 of the indolizine, by transforming the ethyl ester group into the corresponding propargyl-based indolizine derivative suitable for subsequent “click” chemistry.

2. Results and discussions

2.1. Synthesis

Fluorescent pyridyl-indolizine derivative **8** (Scheme 1) was designed as potential DNA binding agents and pH sensitive dyes and synthesized in moderate yield in an adopted four step synthesis based upon our methodological background in the preparation of substituted indolizines.^{4,7}





Scheme 1. Synthesis of compound **8**. Compounds **1** and **3** were reported earlier.^{4a, 7a}

Previously reported monoquateryary 4,4'-dipyridinium phenacyl quaternary salt^{7a} **1** was reacted at room temperature with ethyl propiolate **2** as activated alkyne, in the presence of triethylamine^{4a}. Isolated intermediate indolizine **3** was subsequently hydrolysed into the corresponding carboxylic acid derivative **4**^{7b} which was then reacted with propargyl amine to yield alkyne-substituted indolizine derivative **5**, suitable for further “click” reactions. Separately, chloroanthracene **6** was straightforwardly transformed into corresponding azide **5**.⁸ In the final step, alkyne indolizine **5** was reacted together with azide **5** in a “click” type reaction to yield the final substituted pyridyl-indolizine **8**. All new compounds have been characterized by elemental analysis, ¹H NMR, ¹³C NMR and FTIR. All of the data in the spectra were in good accordance with the designed structures.

2.2. Spectroscopic studies

As shown in previous studies,^{4,9} quite a number of representatives of the class of indolizines are highly fluorescent compounds, some of the indolizines even with remarkably high *Stokes* shift. An investigation of the absorption and emission properties of both the precursor pyridyl-indolizine **5** and the final indolizine **8** in aqueous buffer solutions reveals that the compounds belong to the class of yellow fluorophores (Table 1), having the absorption maxima between 360 and 470 nm and emission maxima between 450 and 600 nm (Fig. 2, 3). The calculation of *Stokes* shifts for buffer solutions also reveals high values, comparable or even higher to the previously reported indolizines in organic solvents.^{4b}

Table 1. UV-vis and fluorescence properties of indolizines **5** and **8** in aqueous buffer at different pH.

	pH	$\lambda_{\text{max,abs}}$ [nm]	$\lambda_{\text{max,em}}$ [nm]	<i>Stokes</i> shift $\Delta\delta$, [cm ⁻¹] ^a
5	2.0	395	521	6123
	5.0		539	6764
	5.5		539	6764
	6.0		539	6764
	6.5		539	6764

	7.0		539	6764
	7.5		539	6764
	8.0		539	6764
	12.0		491, 526	4950, 6305
8	2.0	395	560	7459
	5.0		486, 525	4740, 6269
	5.5		480, 513	4483, 5823
	6.0		480, 514	4483, 5861
	6.5		480	4483
	7.0		480	4483
	7.5		481	4526
	8.0		482	4570
	12.0		482	4570

$$^a) \Delta\tilde{\nu} = 1/\lambda_{\max,\text{abs}} - 1/\lambda_{\max,\text{em}}$$

The absorption and emission spectra were recorded in water after subsequent addition of HCl (0.1M, pH = 2.0) or NaOH (0.1M, pH = 12.0) and in buffer solutions at pH values between 5 and 8 using 1xTAE buffer (40 mM Tris, 20 mM acetic acid and 1 mM EDTA) adjusted to the corresponding pH value by adding acetic acid or trimethylamine (Fig. 2).

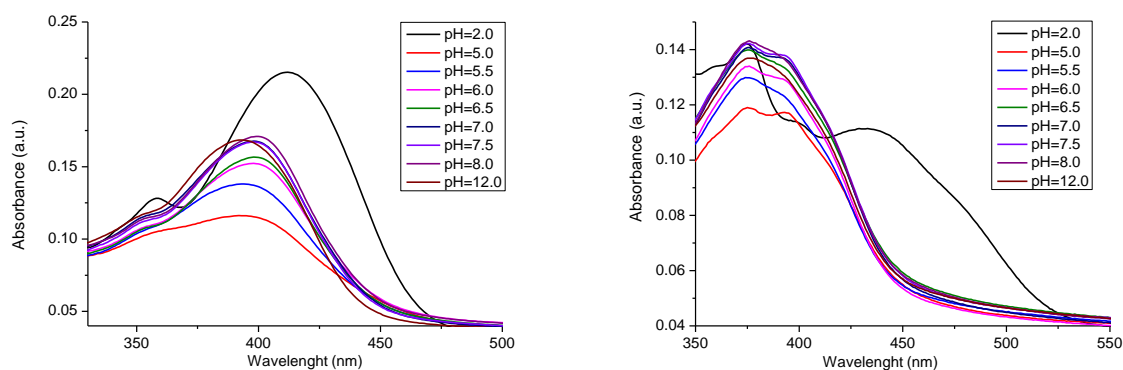


Fig. 2 UV-vis spectra in water for compound **5** (left) and **8** (right) at pH = 2.0 (0.1M, HCl); 5.0; 5.5; 6.0; 6.5; 7.0; 7.5; 8.0; 12.0 (0.1M, NaOH)

Thus, the absorption spectra of indolizine **5** (Fig. 2, left) in water at different pH values exhibit broad bands with a clear maximum at 395 nm, except for the protonated form in 0.1 M HCl, showing two distinct maxima at 358 nm and 415 nm. Indolizine **8** (Fig. 2, right) exhibits structured broad bands, due to the presence of the anthracene moiety, at approximately 380 nm with slight variations in intensity, except for the spectrum in 0.1 M HCl which, due to the fully protonated pyridine substituent also shows a sharper maximum at 370 nm and a broad band at 440 nm.

To investigate the emission properties of compounds **5** and **8**, Stock solutions (1×10^{-3} M) in DMF (HPLC grade) were prepared and then diluted (3×10^{-6} M, 0.3% DMF) with 1xTAE buffer solutions of corresponding pH values. The fluorescence emission was recorded between 425 and 700 nm, with excitation at 395 nm. The emission of precursor compound **5** at acidic pH value of 2.0 is 6-fold stronger than at pH values of 5-12.0 and are similar in behaviour to the pyridyl-indolizines in organic solvents.⁴ We could observe fluorescence emission band with a shoulder at 495 nm at pH of 12.0 and a strong bathochromic shift of the emission maximum to 595 nm at pH values from 8 to 5.0 with small variation in intensity (Fig 3 left). The fluorescence emission spectra under acidic and neutral conditions have similar shapes, except for the band at pH of 12.0 representing the mix of non-protonated and partially protonated species.

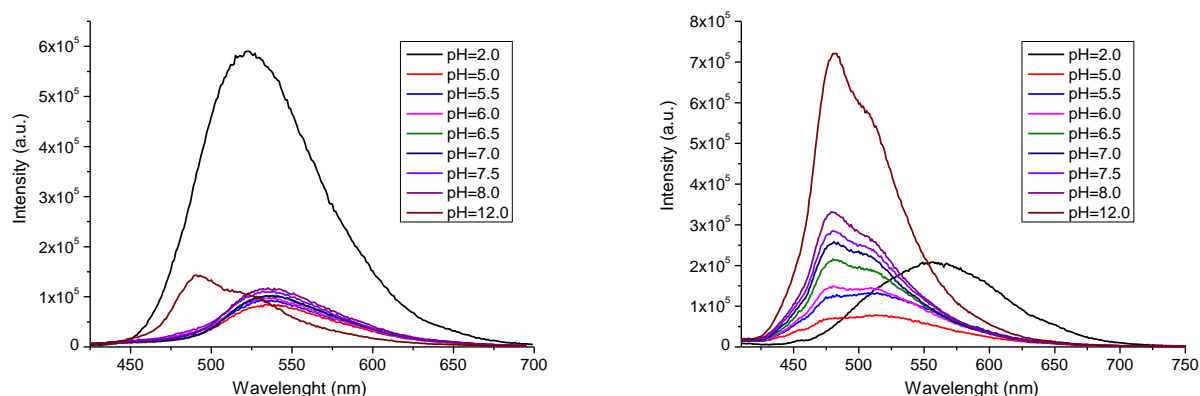


Fig. 3 Fluorescence emission spectra in water and buffer solutions for compounds **5** (left) and **8** (right) at pH = 2.0 (0.1M HCl); 5.0; 5.5; 6.0; 6.5; 7.0; 7.5; 8.0; 12.0 (0.1M NaOH)

Contrarily, the emission spectra of compound **8** in buffer solutions at pH = 5-12 exhibit bands with a shoulder at ca. 475 nm when exciting at $\lambda = 395$ nm. The resulted spectral band is not coincident with the typical emission spectrum of anthracene (vibrationally structured emission between 400 and 500 nm), but is similar in behaviour to previously investigated indolizine (two bands with different intensities depending on the pH value between 420 and 520 nm).⁴ At pH = 12.0, the solution emits strongly in the green spectral window at 475 nm and the fluorescence intensity is 7-fold than at pH = 5.0 (Fig. 3 right). With the decreasing of pH value the fluorescence intensity decreases correspondingly. Interestingly, at pH = 2.0 when the pyridine nitrogen is fully protonated, the fluorescence emission intensity increases by 2-fold in comparison to the emission at pH of 5.0 with important changes in the shape of the band and the emission maximum. Thus, the emission band shape is similar to the band of the protonated pyridyl-indolizines in organic solvents⁴ with the similar bathochromic shift of the maximum to the 570 nm.

2.3. Interactions of **5** and **8** with nucleic acids in aqueous solution

In biological systems, anthracene derivatives bind keenly to DNA¹⁰ where they interact by intercalative and by groove-binding ways.¹¹ This has constituted the basis for their use as chemotherapeutic agents. To investigate the interaction of nucleic acids with pyridine-indolizines **5** and **8**, we performed agarose gel electrophoresis analysis and spectroscopic investigations. Thus, deoxyribonucleic acid, low molecular weight from salmon sperm (sDNA) was used as a natural double-stranded DNA to test the binding properties of compounds **5** and **8** (Fig. 4)

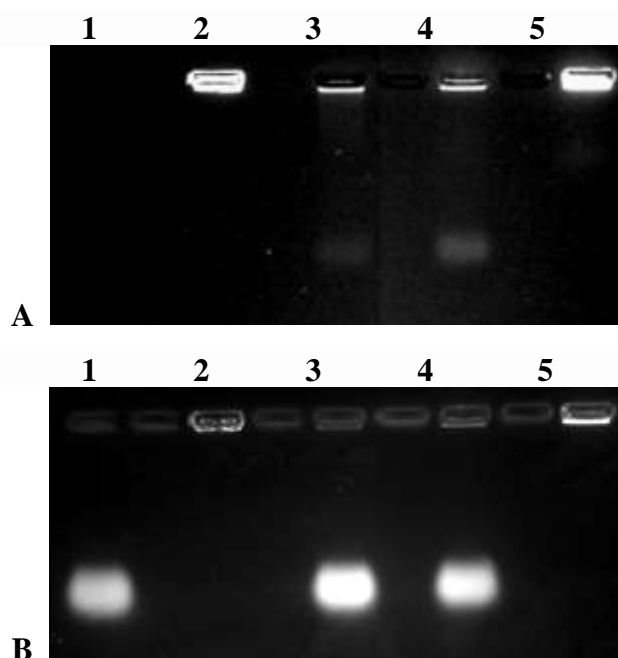


Fig. 4. Photographs of 1% nondenaturing agarose gel showing the interaction of compounds **5** and **8** with sDNA before (**A**) and after (**B**) the developing of the gel with ethidium bromide. Lane 1: salmon sperm DNA; lane 2: compound **5**; lane 3: compound **5** + DNA; lane 4: compound **8** + DNA; lane 5: compound **8**.

The compounds **5** and **8** (5 μ L, 1×10^{-3} M in DMF) were mixed with sDNA water solution (40 μ L, 5mg/mL) and incubated for 24 hours and then electrophoresed on a 1.0% non-denaturing agarose gel. The binding of compounds **5** and **8** with sDNA was visualized at the wavelength of 254 nm using a DNR Bio-imaging system without (Fig. 4 A) and after ethidium bromide staining (Fig. 4 B). From an examination of the gel in Figures 4 A, it is evident that both investigated compounds interact with sDNA yielding low fluorescent migration spots in Lane 3 and Lane 4 corresponding to mixtures of compound **5** and **8** with sDNA. Native compounds didn't show any mobility (Lane 2 and 5) representing fluorescent spots in the pockets of the gel, while native sDNA was not visible under these

conditions. After staining of the same gel with ethidium bromide (Fig. 4 B) the migration reference spot of the sDNA could be visualized (Lane 1) and compared to the similar migration spots of the reaction mixtures in Lane 3 and 4 thus evidencing the DNA-organic compound nature of the fluorescent spots. Notably, the intensity of the sDNA reference spot after staining (Fig.4 B, Lane 1) is weaker when comparing to the spots in Lanes 3 and 4 (spot intensities measured with the software, comparative data not presented) probably due to the combined emissions in corresponding lanes of both sDNA-intercalated ethidium bromide and sDNA-bound compounds **5** and **8**.

UV-visible and fluorescence spectra were acquired next, in order to further examine the interactions of compounds **5** and **8** with sDNA (Fig. 5).

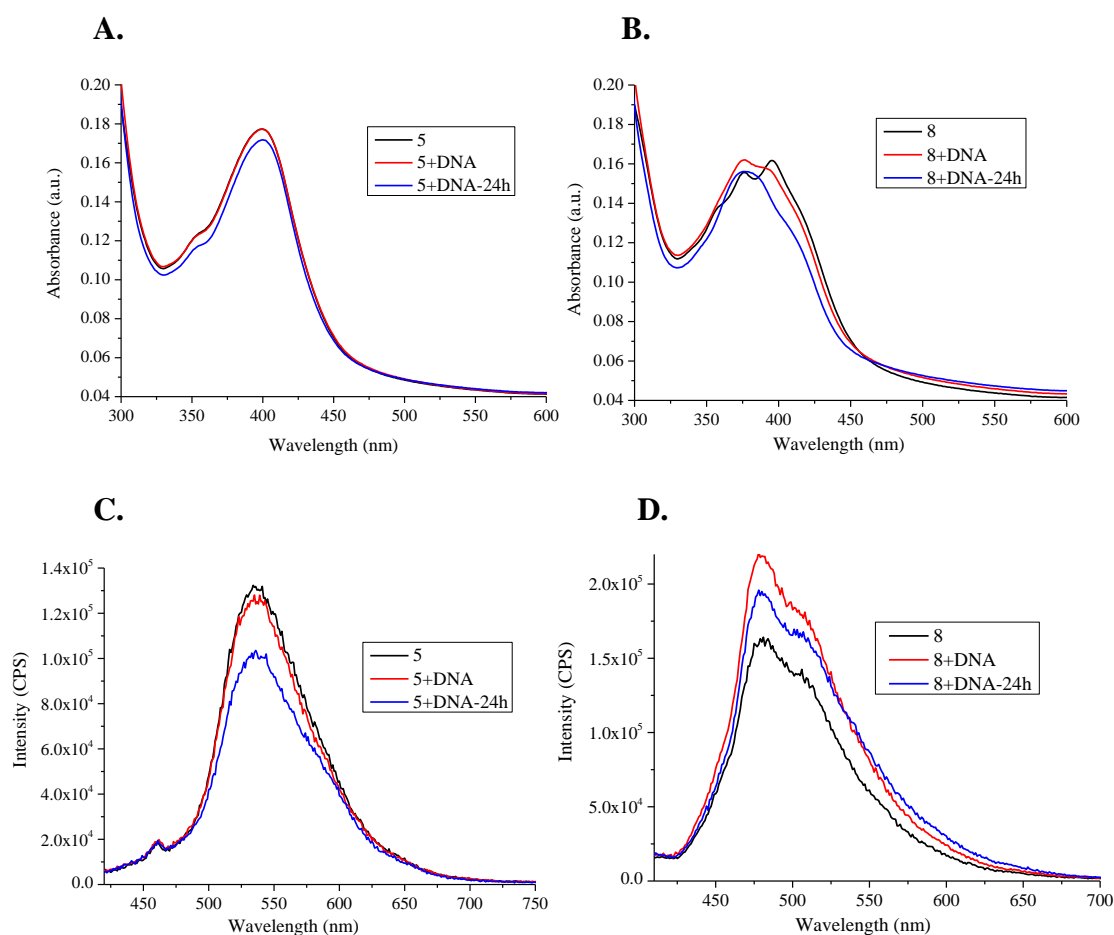


Fig. 5. UV-vis absorbance spectra of compounds **5** (A) and **8** (B) and fluorescence emission spectra of compounds **5** (C) and **8** (D) recorded at 22 °C in 1xTAE buffer pH 7.4 before and after the addition of DNA (0 min and 24 hours).

Compounds **5** and **8** (30 μ L, 1×10^{-3} M in DMF) were dissolved in 1xTAE buffer solution (3 mL, pH 7.4) and the UV-vis absorption spectra were recorded from 600 nm to 300 nm at 22 °C before the addition of sDNA, immediately after the addition of sDNA solution (10 μ L, 5 mg/mL) and after the

incubation of the indolizine-sDNA mixture at room temperature for 24 hours. The absorption spectrum of compound **5** did not show any changes in the shape or intensity of the band immediately after the addition of sDNA (Fig. 5 A), the differences could be observed after 24 hours by the decreasing of the absorption band intensity. Contrarily, upon the addition of sDNA, the absorption spectrum of compound **8** showed instantaneous changes in the shape of the band (Fig. 5 B), the structured band yielded by anthracene suffering modifications and after 24 hours transforming into a broad band with a slightly weaker intensity. These modifications in the shape of the absorption band suggest almost immediate interaction of compound **8** with sDNA. Different behaviour in the interaction of indolizines **5** and **8** with sDNA suggests differences in the interaction mechanisms driven by the compounds structure. Apparently, the presence of the anthracene moiety in the structure of indolizine **8** facilitates easier interaction with nucleic acids due to its higher affinity to DNA molecule when compared to the propargyl moiety of the indolizine **5**. Towards this affirmation come the differences in the emission spectra of the mixtures. In case of compound **5**, addition of sDNA did not produce any significant changes to the initial shape or intensity of the emission band (Fig. 5 C), a difference being observed only after 24 hours of incubation. On the other hand, after the addition of sDNA to the solution of compound **8** under similar experimental conditions, we could observe immediate increase in fluorescence intensity of the mixture (Fig. 5 D), followed by additional increase after 24 hours. We speculate that low fluorescence intensity of compound **8** before the addition of sDNA could be explained by aggregation-caused quenching of anthracene moiety from the structure of **8** in water which is subsequently disrupted in the presence of a biological target, leading to the considerable increase of fluorescence.¹²

2.4. Molecular docking studies

To unveil the differences in binding mechanism of compounds **5** and **8** to DNA, we performed Molecular docking simulation of the corresponding systems. Molecular docking is a computational method applied for predicting noncovalent binding and affinity of macromolecules, or of a macromolecule (receptor) and a small molecule (ligand), starting from their unbound structures.¹³ In this study, for molecular docking simulations we used the AutoDock Vina method¹³ implemented in the YASARA Structure software package.¹⁴ Structures of pyridyl-indolizines **5** and **8** (ligands) were first drawn and optimized at PM3 level of theory using Hyperchem software¹⁵ and then exported to YASARA program. The simulated DNA oligonucleotide (receptor) in this study was the Drew-Dickerson dodecamer d(CGCGAATTCGCG) containing 24 nucleotides, which was built directly by YASARA. The program involves an automatic parameterization procedure (termed “AutoSMILES”) for the unknown structures, the algorithm was employed to generate force field parameters for the receptor DNA and ligands (compounds **5** and **8**). All molecular simulations were done using the self-

parameterizing knowledge-based YASARA force field.¹⁶ Before molecular docking simulation, the energy minimization was performed on the structures of receptor (DNA) and ligands. Thus, the unbound structures (i.e. starting conformers) of receptor and ligands were first optimized considering the implicit water solvent at pH 7.4. During molecular docking simulations, the receptor was treated as rigid structure, whereas ligands were treated as flexible molecules. The computations (by VINA) were performed using a number of 100 docking runs followed by the cluster analysis. Commonly, docking results are grouped around certain hot spot conformations, and the lowest energy complex in each cluster is saved by YASARA program. Note that, two complexes belong to different clusters if the ligand RMSD (root-mean-square-deviation) is larger than an imposed minimum value. In this work, we maintained a cluster RMSD (for heavy atoms) equal to 5 Å. After clustering the 100 runs, distinct complex conformations were found and grouped into 7 clusters and 9 clusters for the ligands **8** and **5**, respectively. These results suggested the multiple hotspots for binding and for each complex conformer the binding energy and dissociation constant were determined. The VINA molecular docking simulation results predicted the most probable conformations of complexes between DNA (receptor) and indolizines **5** and **8** as shown in Fig.6.

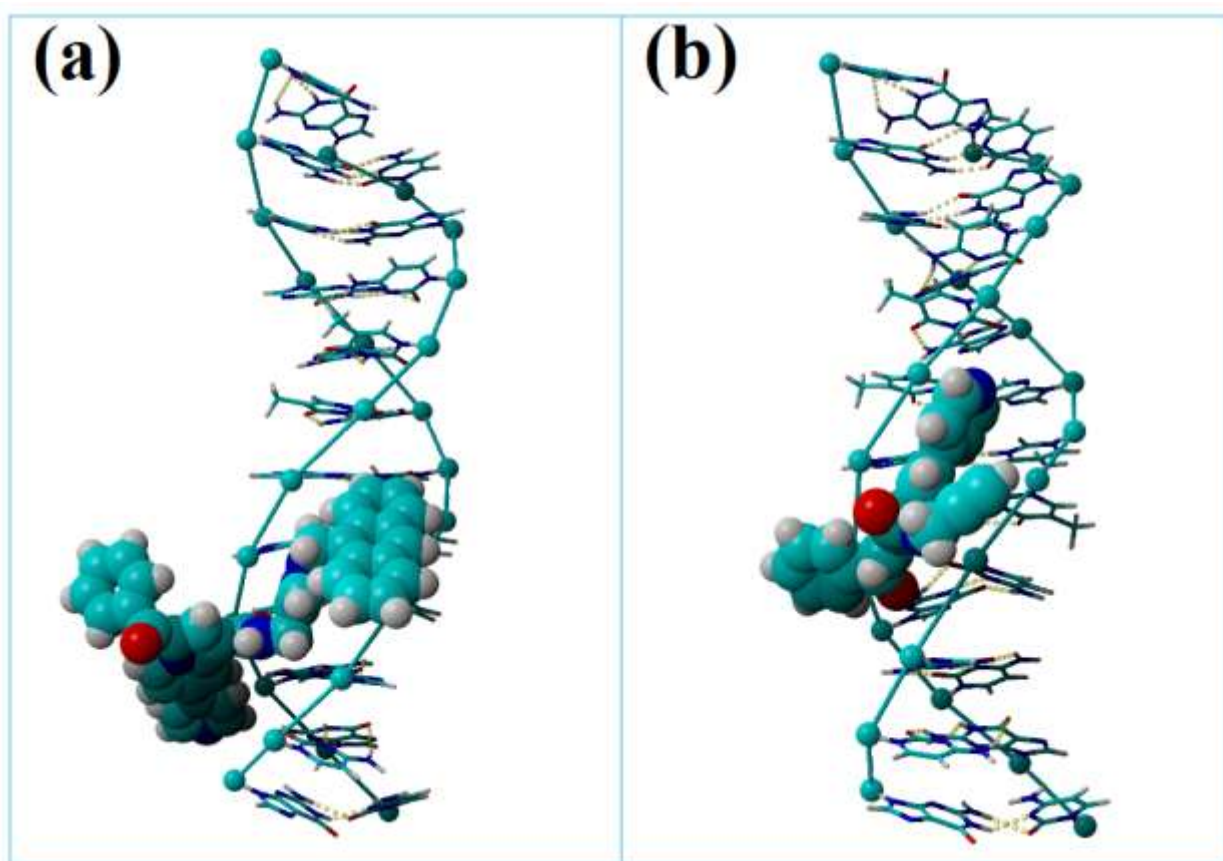


Fig. 6. Docking structures of the complexes between: (a) DNA oligonucleotide (receptor) and indolizine **8** (ligand): $E_b = -9.87$ kcal/mol and $K_d = 58.138$ nM; (b) DNA oligonucleotide (receptor) and indolizine **5** (ligand): $E_b = -7.60$ kcal/mol and $K_d = 2681.6$ nM.

The values of calculated binding energy E_b and dissociation constant K_d were as follows: 1) $E_b = -9.87$ kcal/mol and $K_d = 58.138$ nM, for DNA-ligand (**8**) complex (see Fig.1a), and 2) $E_b = -7.60$ kcal/mol and $K_d = 2681.6$ nM, for DNA-ligand (**5**) complex (see Fig.1b). These results suggest that the anthracene-modified indolizine **8** has a superior affinity for the receptor (DNA) than its precursor indolizine **5**, due to much lower values of binding energy and dissociation constant of the corresponding complex. As can be seen in Fig.1, both indolizines **5** and **8** were bound to DNA receptor at minor groove via hydrophobic interactions. According to Fig.1a, the following groups of the ligand **8** were imbedded into the minor groove of DNA: pyridine moiety, peptide group, triazole and part of anthracene group. Similarly, for the ligand **5**, the groups connected to the minor groove of DNA were: pyridine and peptide group (Fig.1b). In both cases, the phenacyl group from position 3 of the indolizinic ring of the ligands (**5** and **8**) was positioned outside the minor groove of the receptor.

3. Conclusions

In summary, a new 7-(pyridin-4-yl)-substituted indolizine derivative containing an anthracene moiety with pH dependent emission properties and nucleic acid binding properties was designed and synthesized. The absorption and fluorescence comparative studies of both the final compound and its precursor containing pyridine-indolizinic skeleton were performed in buffer solutions at different pH values. Both compounds showed very particular absorption and emission behaviour, depending on the pH value and the structure of investigated indolizines. Interestingly, presented indolizine derivatives bind to DNA at physiological pH, the fact proved by changes in absorption and emission spectra before and after the addition of targeted DNA and by gel electrophoresis experiments. Additionally, to get a deeper insight into interaction mechanisms of indolizines **5** and **8** and double-stranded DNA we performed molecular docking simulations using AutoDock Vina method from YASARA software package. Simulation results revealed that indolizine **8** containing an anthracene moiety has a much better affinity for DNA than the indolizine **5** containing only pyridine-indolizine moiety, owing to lower values of binding energy and dissociation constant of the complex, data that correlate to the absorption and emission experimental data. Our future efforts will be focused on optimizing the structure of the indolizine-based nucleic acid binders containing anthracene moiety and in deep studies on the binding mechanisms, followed by DNA photocleavage experiments which should unveil the potential of anthracene modified indolizine derivatives as anticancer drugs.

4. Experimental section

4.1. Chemicals and starting materials

All commercially available reagents were used without further purification. All chemicals were purchased in their highest purity grade. Deoxyribonucleic acid, low molecular weight from salmon sperm (salmon sperm DNA) was purchased from Sigma Aldrich as lyophilized powder and used in the

experiment as a 5 mg/mL stock solution. Solvents used for the spectrometric studies were of spectroscopic grade.

4.2. Measurements

Melting points were recorded on an A. Krüss Optronic Melting Point Meter KSPI and are uncorrected. Proton and carbon nuclear magnetic resonance (δ_H , δ_C) spectra were recorded on a DRX-500 Bruker (500 MHz) with tetramethylsilane (TMS) as an internal standard. IR spectra were recorded on a FTIR Shimadzu or Jasco 660 *plus* FTIR spectrophotometer. UV-vis spectra were recorded on a Lambda 35, Perkin Elmer spectrometer. Fluorescence measurements were carried out using an Fluoromax4, Horiba fluorescence spectrophotometer. Agarose gel electrophoresis assay for determining the binding of **5** and **8** with salmon sperm DNA was performed as follows: 10 μ L (10 mM) of **5** or **8** were mixed together with 5 μ L (10mg/mL) salmon sperm DNA in 1xTAE buffer (40 mM Tris, 20 mM acetic acid and 1 mM EDTA, pH = 7.4) and incubation for 24h at 25°C. Sucrose (5 μ l with conc. 25% in water) was added and the samples were immediately loaded onto 1% agarose gel and run at 90 mV for 60 minutes at room temperature in 1xTAE buffer. Subsequently, the gels were imaged without staining and then stained with ethidium bromide for 10 minutes at room temperature and then photographed. The gels were visualized and analyzed at the wavelength of 254 nm using a DNR Bio-imaging system.

4.3. Synthesis and characterization of compounds

The synthetic route followed for the compounds **3** and **4** is shown in Scheme 1 and is based on reported methods^{4a, 7b}. The detailed procedures and the spectral data obtained from the characterization of the new compounds are described below.

4.3.1. Synthesis of 3-benzoyl-7-(pyridin-4-yl)indolizine-1-carboxylic acid (4). Ethyl 3-benzoyl-7-(pyridine-4-yl) indolizine-1-carboxylate **3** (2.1 mmol) was hydrolysed in EtOH:MeOH:4M KOH (25:25:8, 150 ml) at 60°C for 3 h. After cooling, the reaction mixture was poured into ice water (100 ml) and acidified by slow addition of 10% citric acid until pH 6. The resulted solid was separated by filtration and dried to give 3-benzoyl-7-(pyridine-4-yl)indolizine-1-carboxylic acid **4** as a yellow solid, which was used in the next step without any further purification due to the poor solubility in common solvents. Yield: 95%. m.p. 300-302 °C. FTIR (KBr, cm^{-1}): 3200-2500, 1605, 128, 1381, 1228. ^1H NMR (500 MHz, DMSO- d_6), δ (ppm): 7.57 (d, J = 7.0 Hz, 2H), 7.63 (t, J = 7.0 Hz, 1H), 7.70 (s, 1H), 7.81 (overlapped signals, 3H), 8.54 (d, J = 4.5 Hz, 2H), 8.86 (s, 1H), 9.04 (d, J = 4.5 Hz, 2H), 9.01 (d, J =6.5 Hz, 1H). ^{13}C -NMR (125 MHz), δ (ppm): 109.4 (1C), 113.9 (1C), 119.1 (1C), 123.2 (1C), 124.7 (2C), 128.8 (2C), 128.9 (1C), 129.2 (2C), 129.5 (1C), 132.3 (1C), 132.9 (1C), 138.5 (1C), 139.3 (1C), 142.8 (2C), 153.6 (1C), 164.7 (1C), 171.6 (1C), 185.3 (1C). Calculated for $\text{C}_{21}\text{H}_{14}\text{N}_2\text{O}_3$: %C 73.68; %H 4.12; %N 8.18. Experimental: %C 73.70; %H 4.04; %N 8.22.

4.3.2. *Synthesis of 3-benzoyl-N-(prop-2-yn-1-yl)-7-(pyridin-4-yl)indolizine-1-carboxamide (5)*. To a solution of 3-benzoyl-7-(pyridine-4-yl)indolizine-1-carboxylic acid (0.27 mmol, 1 equiv., 0.09 g) in 5 ml of chloroform were added 0.04 g (0.30, mmol, 1.1 equiv.) of oxalyl chloride and catalytic amount of DMF. After 24 h at reflux, the solvent and excess oxalyl chloride were removed in vacuo to afford the corresponding indolizinylyl chloride, which was used in the next step without any further purification. Thus, propargyl amine (0.34 mmol, 1.25 equiv., 0.2 mL) and TEA (0.81 mmol, 3 equiv., 0.1 ml) were added to 7ml of chloroform, and the obtained suspension is stirred under nitrogen at rt for 20 min. The acyl chloride dissolved in 5 ml of chloroform was added dropwise over 15 min (magnetic stirring), and the resulting mixture was then stirred over night at rt. The solid was collected by filtration to give a solid which was then washed with methanol and dried to give the corresponding compound **5**. Yield: 52%. m.p. 346-350 °C. FTIR (KBr, cm⁻¹): 3285, 1651, 1530, 1406, 1235. ¹H NMR (500 MHz, DMSO-d₆), δ(ppm): 3.13 (bs, 1H), 4.06 (ad, J= 3.0 Hz, 2H), 7.60 (t, J= 7.5 Hz, 2H), 7.67 (t, J= 7.5 Hz, 1H), 7.72(d, J= 7.0 Hz, 1H), 7.84 (d, J= 7.5 Hz, 2H), 7.86 (d, J= 4.5 Hz, 2H), 8.14 (s, 1H), 8.74 (d, J= 5.0 Hz, 2H), 8.91 (t, J= 5.0 Hz, 1H), 8.96 (as, 1H), 9.90 (d, J= 7.5 Hz, 1H). ¹³C-NMR (125 MHz), δ(ppm): 34.0 (1C), 72.9 (1C), 81.5 (1C), 110.0 (1C), 113.8 (1C), 116.9 (1C), 121.0 (2C), 121.7 (1C), 126.0 (1C), 128.6 (2C), 128.7 (1C), 129.0 (2C), 131.7 (1C), 135.2 (1C), 138.8 (1C), 139.3 (1C), 144.4 (1C), 150.6 (2C), 162.9 (1C), 184.6 (1C). Calculated for C₂₄H₁₇N₃O₂: %C 75.97; %H 4.52; %N 11.08. Experimental: %C 75.92; %H 4.46; %N 11.14.

4.3.3. *Synthesis of 9-(azidomethyl)anthracene (7)*.⁸ A mixture of 9-(chloromethyl)anthracene (4.41 mmol) and sodium azide (6.62 mmol) in 30 mL of MeCN was refluxed for 5 h. After completion of the reaction, the solvent was removed under reduced pressure and the resulting solid was recrystallized from CH₂Cl₂/methanol mixture to give compound **7**.

4.3.4. *Synthesis of N-((1-(anthracen-9-ylmethyl)-1H-1,2,3-triazol-4-yl)methyl)-3-benzoyl-7-(pyridin-4-yl)indolizine-1-carboxamide (8)*. Azide **7** (0.03 g, 1 equiv., 0.13 mmol) was dissolved in chloroform (5 mL). Then, alkyne **5** (0.05 g, 1 equiv. 0.13 mmol) and triethylamine (0.1 mL) were added and the resulting reaction mixture was degased. CuI (2.5 mg, 0.1 equiv.) was added and the resulting mixture was stirred at reflux for 24 hours. After cooling at room temperature, the formed solid was filtered and dried. Yield: 62%. m.p. 335-340 °C. FTIR (KBr, cm⁻¹): 1611, 1541, 1460, 1342, 1236. ¹H NMR (500 MHz, DMSO-d₆), δ(ppm): 4.40 (s, 2H), 6.60 (s, 2H), 7.52-7.66 (m, 10H), 7.75 (d, J= 7.0 Hz, 2H), 7.87 (as, 2H), 8.00 (s, 1H), 8.12 (d, J= 8.0 Hz, 2H), 8.59 (d, J=9.0 Hz, 2H), 8.70 (s, 1H), 8.84 (as, 2H), 8.94 (s, 1H), 9.81 (d, J= 5.0 Hz, 1H). ¹³C-NMR (125 MHz), δ(ppm): 34.0 (1C), 45.4 (1C), 110.0 (1C), 113.0 (1C), 116.0 (1C), 120.5 (2C), 121.4 (1C), 124.0 (3C), 125.3 (2C), 125.8 (1C), 125.9 (2C), 127.0 (3C), 128.4 (3C), 128.7 (1C), 128.8 (2C), 129.0 (4C), 130.2 (1C), 131.0 (1C), 131.5 (1C), 138.9 (1C), 139.3 (1C), 150.6 (2C), 163.1 (1C), 184.5 (1C). Experimental: %C 76.40; %H 4.55; %N 13.78.

Acknowledgments

This work was supported by a grant of the Romanian National Authority for Scientific Research and Innovation, CNCS – UEFISCDI, project number PN-II-RU-TE-2014-4-1444 and H2020 ERA Chairs Project no. 667387: SupraChem Lab Laboratory of Supramolecular Chemistry for Adaptive Delivery Systems ERA Chair initiative.

References and notes

1. (a) Du, Y. H.; Huang, J.; Weng, X. C.; Zhou, X. *Curr. Med. Chem.* **2010**, *17*, 173; (b) Bischoff, G.; Hoffmann, S. *Curr. Med. Chem.* **2002**, *9*, 321; (c) Banerjee, S.; Veale, E. B.; Phelan, C. M.; Murphy, S. A.; Tocci, G. M.; Gillespie, L. J.; Frimannsson, D. O.; Kelly, J. M.; Gunnlaugsson, T. *Chem. Soc. Rev.* **2013**, *42*, 1601; (d) Schaferling, M. *Angew. Chem. Int. Ed.* **2012**, *51*, 3532.
2. (a) Kazmierska, A.; Gryl, M.; Stadnicka, K.; Sieron, L.; Eilmes, A.; Nowak, J.; Matkovic, M.; Radic-Stojkovic, M.; Piantanida, I.; Eilmes, J. *Tetrahedron* **2015**, *71*, 4163; (b) Tronconi, M.; Colombo, A.; De Cesare, M.; Marchesini, R.; Woodburn, K. W.; Reiss, J. A.; Phillips, D. R.; Zunino, F. *Cancer Lett.* **1995**, *88*, 41; (c) Van Vliet, L. D.; Ellis, T.; Foley, P. J.; Liu, L.; Pfeffer, F. M.; Russell, R. A.; Warren, R. N.; Hollfelder, F.; Waring, M. J. *J. Med. Chem.* **2007**, *50*, 2326; (d) Xue, L.; Xi, H.; Kumar, S.; Gray, D.; Davis, E.; Hamilton, P.; Skriba, M.; Arya, D. P. *Biochemistry* **2010**, *49*, 5540; (e) Samanta, S. K.; Dutta, D.; Roy, S.; Bhattacharya, K.; Sarkar, S.; Dasgupta, A. K.; Pal, B. C.; Mandal, C.; Mandal, C. *J. Med. Chem.* **2013**, *56*, 5709; (f) Rahman, K. M.; Jackson, P. J. M.; James, C. H.; Basu, B. P.; Hartley, J. A.; de la Fuente, M.; Schatzlein, A.; Robson, M.; Pedley, R. B.; Pepper, C.; Fox, K. R.; Howard, P. W.; Thurston, D. E. *J. Med. Chem.* **2013**, *56*, 2911.
3. (a) Lavis, L. D.; Raines, R. T. *ACS Chem. Biol.* **2008**, *3*, 142; (b) Fan, J.; Hu, M.; Zhan, P.; Peng, X. *Chem. Soc. Rev.*, **2013**, *42*, 29.
4. (a) Rotaru, A.; Avram, E.; Druta, I.; Danac, R. *Arkivoc* **2009**, *13*, 287; (b) Rotaru, A.; Druta, I.; Oeser, T.; Müller, T. J.J. *Helvetica Chimica Acta* **2005**, *88*, 1798.
5. Kim, E.; Lee, Y.; Lee, S.; Park, S. B. *Acc. Chem. Res.*, **2015**, *48*, 538.
6. (a) Kobayashi, K.; Endo, K.; Aoyama, Y.; Masuda, H. *Tetrahedron Lett.*, **1993**, *34*, 7929; (b) Mizobe, Y.; Tohnai, N.; Miyata, M.; Hasegawa, Y. *Chem. Commun.*, **2005**, 1839; (c) Yoshizawa, M.; Klosterman, J. K. *Chem. Soc. Rev.* **2014**, *43*, 1885; (d) Kumar, C. V.; Punzalan, E. H. A.; Tan, W. B. *Tetrahedron* **2000**, *56*, 7027.

7. (a) Rotaru, A.; Danac, R.; Druta, I. *Journal of Heterocyclic Chemistry* **2004**, *41*, 893; (b) Danac, R.; Rusu, R.; Rotaru, A.; Pui, A.; Shova, S. *Supramol. Chem.* **2012**, *24*, 424.
8. Chang, K. C.; Su, I. H.; Senthilvelan, A.; Chung, W. S. *Org. Lett.*, **2007**, *9*, 3363.
9. (a) Vlahovici, A.; Andrei, M.; Druta, I. *J. Lumin.* **2002**, *96*, 279; (b) Vlahovici, A.; Druta, I.; Andrei, M.; Cotlet, M.; Dinica, R. *J. Lumin.* **1999**, *82*, 155; (c) Sonnenschein, H.; Hennrich, G.; Resch-Genger, U.; Schulz, B. *Dyes Pigments* **2000**, *46*, 23.
10. (a) Bowden, G. T.; Roberts, R.; Alberts, D. S.; Peng, Y. M.; Garcia, D. *Cancer Res.* **1985**, *45*, 4915; (b) Iyengar, B. S.; Dorr, R. T.; Alberts, D. S.; Sólyom, A. M.; Krutzsch, M.; Remers, W. A. *J. Med. Chem.* **1997**, *40*, 3734.
11. (a) Wilson, W. D.; Wang, Y. H.; Kusuma, S.; Chandrasekaran, S.; Boykin, D. W. *Biophys. Chem.* **1986**, *24*, 101; (b) Modukuru, N. K.; Snow, K. J.; Perrin, B. S.; Bhambhani, A.; Duff, M.; Kumar, C. V. *J. Photochem. Photobiol. A* **2006**, *177*, 43; (c) Tan, W. B.; Bhambhani, A.; Duff, M. R.; Rodger, A.; Kumar, C. V. *Photochem. Photobiol.* **2006**, *82*, 20.
12. (a) Suzuki, Y.; Yokoyama, K. *J. Am. Chem. Soc.* **2005**, *127*, 17799. (b) Royer, C. A. *Chem. Rev.* **2006**, *106*, 1769.
13. Trott, O.; Olson, A. J. *J. Comput. Chem.* **2010**, *31*, 455.
14. YASARA, Yet Another Scientific Artificial Reality Application: Molecular graphics, modeling and simulation program, official web-site: <http://www.yasara.org/>
15. HyperChem(TM) Release 8.0, Hypercube, Inc., 1115 NW 4th Street, Gainesville, Florida 32601, USA, official web-site: <http://www.hyper.com/>
16. (a) Krieger, E.; Koraimann, G.; Vriend, G. *Proteins* **2002**, *47*, 393; (b) Krieger, E.; Joo, K.; Lee, J.; Lee, J.; Raman, S.; Thompson, J.; Tyka, M.; Baker, D.; Karplus, K. *Proteins* **2009**, *77*, 114.